Using UAV and VBS-RTK for Rapid Reconstruction of Environmental 3D Elevation Data of the Typhoon Morakot Disaster Area and Disaster Scale Assessment

Chien-Ting Wu[1]* Cheng-Yang Hsiao[2] Pao-Shan Hsieh[2]

ABSTRACT In recent years, typhoons and heavy rains in Taiwan are often accompanied by sediment disasters such as landslides and debris flows. If disaster area information can be obtained in the shortest possible period of time for rapid assessment of sediment transport and disaster scale, it can provide quantitative reference information for follow-up disaster relief and decision-making. Focusing on the Leye collapse in the Typhoon Morakot disaster area and its surroundings as the research area, this study employed UAV, which defies ground photography angle limits and performs low-altitude photography of the disaster-hit area. Next, by using unconventional photogrammetry technology, a field of computer vision technology, combined with VBS-RTK technology, which has become mature in recent years, this study aims to accomplish real time positioning of the reference control points and rapidly reconstruct the environmental 3D elevation data of the disaster area. The proposed approach can enable a rapid quantitative assessment of major sources of sediment, potential unstable areas, and the scale of the sediment disaster. Topographic data obtained using the proposed method can be applied to rapidly calculate landslide depth, and landslide volume after comparison with pre-disaster DTM data.

Key Words : 3D Reconstruction, Unmanned Aerial Vehicles (UAV), VBS-RTK.

1. Introduction

Unmanned Aerial Vehicles (UAV) have the advantages of high mobility, high-resolution, and can be equipped with a still or video camera. Images with geodetic coordinates can be obtained by geometric correction processing of the still images, which can be integrated and overlaid with existing topographic maps, aviation photos, or satellite images. In addition to understanding the disaster situation in the disaster area in a short period of time, operators can operate in a safe and secure location, while saving labor in the current survey of watershed or sediment disaster areas. With rapid access to information using this approach, a large number of photos can be obtained in a short period of time, and the processed data can provide quantitative reference data, rendering it very convenient for post-disaster preliminary investigations. If using these photo data for 3D reconstruction, appropriate control points should be designated within the photos.

Traditional single reference station RTK, in the case of a short base line (6-10 km), can achieve centimeter positioning accuracy. However, the main problem in RTK application is effective distance resulting from the correction data of the reference station. To overcome the operational distance shortcomings of the traditional RTK technology, the study on Virtual Reference Station Systems (Landau et al. 2004) developed a technology using GPS Virtual Reference Station (VRS). National Land Surveying and mapping Center (NLSC) has proposed the e-GPS network RTK technology. In e-GPS network RTK technology, the single GPS base station error model is replaced by the regional GPS multiple base station network error model. The GPS network, consisting of multiple base stations, is used to assess the GPS error model of the area covered by the base station in order to establish the Virtual Base Station (VBS) model for data observation, which provides RTK users in the region with

〔1〕Department of Civil Engineering, National Chiao Tung University, 1001 University Road, Hsinchu, 300, Taiwan, R.O.C.
〔2〕Disaster Prevention Technology Research Center, Sinotech Engineering Consultants, Inc, Taiwan, R.O.C.
* Corresponding Author. E-mail : Kenwu@uch.edu.tw

a main station. The observation data of the VBS will be highly correlated to the error model used by RTK users for data observation. Therefore, after the Virtual Base Station Real Time Kinematic Positioning (VBS-RTK) processing, system errors can be eliminated and RTK positioning accuracy can be improved.

For the requirement of providing high precision real time positioning and expanding the RTK effective operational range, NLSC has established high speed and broadband data transmission technology, via the Internet, and established the national e-GPS system. By using continuous positioning observation data to construct a regional positioning error interpolation model, coupled with VBS-RTK, high accuracy positioning results can be achieved.

Therefore, this study applies VBS-RTK combined with UAV photography to realize rapid and high precision achievements. This study discusses the methods of combining two technologies, uses actual land sediment disaster measurement data for research, and analyzes the errors and effectiveness after the integration of the two technologies.

2. Literature Review

1. VBS-RTK precision performance

As the horizontal accuracy of the present Global Positioning System (GPS) satellite positioning reference network and Virtual Base Station Real Time Kinematic Positioning (VBS-RTK) is about 2 cm, and the elevation accuracy of the present GPS satellite positioning reference network and VBS-RTK is about 5 cm (Wang et al. 2006), its positioning precision can be applied in various fields. Moreover, since the wireless communications and Internet transmission speed is increasingly fast and the broadband is increasing large, RTK technology has become the mainstay of international positioning technology, and advanced countries in the world are actively building systems based on RTK technology.

Wang et al. explicitly pointed out that the Land Survey Bureau of the Ministry of the Interior has been planning high speed and broadband Internet data transmission technology to expand the effective operational range of RTK and reduce main station distribution density. In 2006, the national e-GPS satellite positioning measurement baseline network was established, which uses continuous positioning observation data, constructs a regional positioning error interpolation model and VBS-RTK technology to obtain high precision positioning results, and provides multiple target positioning services and value-added applications Chu and Chien (2004) conducted a case study of a VRS network in Changhua County to analyze results and precision by selecting the 20 known GPS satellite points of the Ministry of Interior. According to the comparison of the GPS VRS measurement results and the original coordinates of the inspection points, the average difference of horizontal coordinates was 1.3 cm and the average difference of the vertical coordinates was 1.3 cm.

From April 2005 to December 2006, NLSC used VBS-RTK positioning technology to conduct four tests of the positioning service networks in northern and central regions and Hualien. VBS-RTK static interpolation positioning precision tends to increase over increasing distances between rovers and major base stations, in particular, deterioration in terms of elevation is particularly apparent. For example, at a distance of 18 km from the major base station, the horizontal average positioning precision can be 2 cm, and the elevation average precision can be 5 cm; however, when the distance is above 32 km, the precision will deteriorate with the increased distance (Wang et al. 2006).

2. Unconventional photogrammetry technology

Due to the time-critical urgency of natural disasters or major accident relief, in recent years, the international community has focused on the study of “unconventional photogrammetry” measurement methods and processes that can be applied in emergency relief (Ko et al. 2010). The method has fewer limits as compared with photogrammetry. For example, it can use the real time disaster site photos provided by residents or media, as well as photos taken by uncalibrated cameras. Sun et al. (2006) and Zhao et al. (2004) used a consumer digital camera to obtain the 3D topographic reconstruction effects of engineering survey accuracy level through the Multiple View Geometry in Computer Vision. At the Cross-Strait Unconventional Photogrammetry Seminar held in National Cheng Kung University in 2010, a research team from the mainland Wuhan University shared the complete processes of data access, processing, and results presentation by unconventional photogrammetry on May 12, 2008 of the Wencuang Earthquake, as the aerial flight was not regularly designed (Fig. 1(a)) due to high time-critical requirements of disaster relief in case of wide and unconfirmed disaster sites (Fig. 1(b)) (Ko et al. 2010), (Zhang

and Ko 2010), (Sun and Duan 2010). In Taiwan, after the Tai Po Shun slope collapse on Highway 3, (Hsiao et al. 2011) used the unconventional photogrammetry technology of computer vision to study the topographic elevation changes in the collapsed area. The error between the measurement results and the high precision GPS on-site measurement results, in terms of elevation, was not more than 16cm.

3. Research Method

1. 3D reconstruction technology

At present, common 3D reconstruction technologies mainly include traditional measurements, aerial, ground and airborne LiDAR, close-range photogrammetry, and unconventional photogrammetry in the field of computer vision technology, which is an emerging application and current research trend. Many scholars have published journals in various application fields, including static image segmentation and combination, document analysis and recognition, intelligent transportation navigation systems, image comparison and video surveillance, and 3D reconstruction (Doermann 1998), (Bunke and Wang 1997), (Masaki 1992), (Bertozzi and Broggi 1997), (Broggi et al. 1999), (Lowe 1999; Lowe 2004; Lowe 2007), (Sun et al. 2006), (Snavely et al. 2010), (Hsiao et al. 2011). 3D reconstruction is actually consistent with the requirements of unconventional photogrammetry. In addition to having fewer limits, as compared with photogrammetry, photos taken by different uncalibrated cameras can be used. Hence, this study uses computer vision unconventional photogrammetry technology for 3D reconstruction.

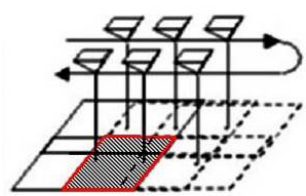

Fig.1(a) Traditional Photogrammetry

Fig.1(b) Unconventional Photogrammetry

In general, coordinated records by UAV often have a large deviation, and there is almost no coordinates for reference in images taken by local residents and investigators. However, 3D reconstruction using photos requires the location of the camera and photographic parameters. This study used images taken by UAV and consumer digital cameras with EXIF (EXchangeable Image file Format) without information regarding camera location. Hence, this study used the key self-calibration technology of "SfM" (Structure from Motion), which is undergoing research in the computer vision field, and has the advantage of no requirements of predetermination of coordinates. First proposed by Tomasi and Kanad (1991), they put all the coordinates of matched features tracked through several frames into a matrix and prove that under orthographic projection this matrix is of rank 3. Then singular-value decomposition is utilised to factor this matrix into two matrices, which represent observed scene and camera motion respectively. Based on this factorization method, many researchers achieve a lot of improvements and progresses, which make the whole processing of SfM more precise, but also at the same time more complex and time consuming. SfM has three major tasks: first, to analyze the movement of the camera and shooting targets; second, the restoration of the camera movement trajectory; finally, to create a three-dimensional scene of the target (Zhou 2010) as shown in Fig. 2. SfM assumes the shooting object is stationary, the shooting object coordinate system, and two or more of the camera coordinate systems as shown in Fig. 3 are in a linear corresponding relationship, which can be described by the coordinate conversion matrix. The mathematical expression for transforming a camera coordinate system to an object coordinate system is expressed as Equation 1 and Equation 2. Where X, Y and Z are the $K1$ camera coordinates and X', Y' and Z' are the $K2$ camera coordinates. At the same time, the coordinate systems of the two cameras must have the relationships of translation (t) and rotation (R), as shown in Equation 3. If sufficient matching points can be determined in the photos, the coordinate conversion matrices of two cameras can be calculated by using such matching points to determine the relative relationship of the camera coordinate systems, R and t, respectively. Then, the relative coordinates of the object can be calculated using the coordinates of the camera position and various matching points in the camera coordinate system.

$$\begin{bmatrix} X_i \\ Y_i \\ Z_i \end{bmatrix} = +R_1 \begin{bmatrix} X \\ Y \\ Z \end{bmatrix} \quad (1)$$

$$\begin{bmatrix} X_i \\ Y_i \\ Z_i \end{bmatrix} = +R_2 \begin{bmatrix} X' \\ Y' \\ Z' \end{bmatrix} \quad (2)$$

$$\begin{bmatrix} X \\ Y \\ Z \end{bmatrix} = +R \begin{bmatrix} X' \\ Y' \\ Z' \end{bmatrix} + t \quad (3)$$

First, the SIFT algorithm, which can recognize matching points by images according to changes in color, contrast, and relative position in different photos, is used for feature points marking and image matching (Lowe 1999; Lowe 2004; Lowe 2007).

Second, the eight-point algorithm is an algorithm used in SfM to estimate the essential matrix or the fundamental matrix related to a stereo camera pair from a set of corresponding image points. Each point pair contributes with one constraining equation on the element in Essential matrix. Since Essential matrix has five degrees of freedom it should therefore be sufficient with only five point pairs to determine Essential matrix. Though possible from a theoretical point of view, the practical implementation of this is not straightforward and has to rely on solving various non-linear equations. According to SfM and image matching results, the relative position of each photo when the image was recorded are calculated.

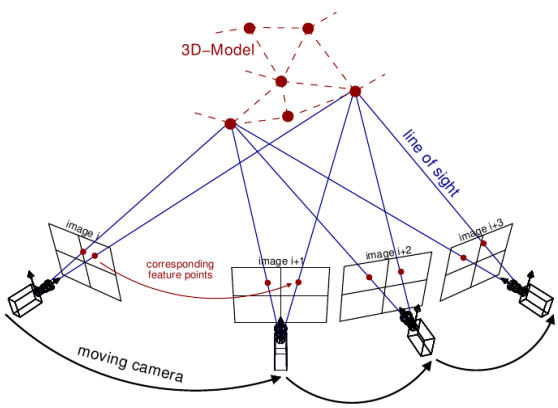

Fig.2 SfM program schematic diagram (Zhou 2010)

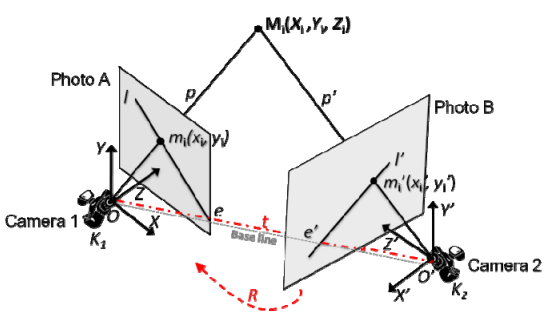

Fig.3 Epipolar geometry of a stereo pair

The third step uses Multi-View Stereopsis (MVS), as proposed by Furukawa and Ponce (2010), which is the optimal approach for effectively increasing point cloud density in order to calculate the 3D point cloud data with the RGB color code. The MVS implements multi-view stereopsis as a simple match, expand, and filter procedure. The match algorithm detects corner and blob features in each image using the Harris and Difference-of-Gaussian (DoG) operators. At the stage of expansion, we add new neighbors to existing patches until they cover the surfaces visible in the scene iteratively. The filtering steps are applied to the reconstructed patches to further enforce visibility consistency and remove erroneous matches.

Finally, as performed in SfM, a 3D reconstruction is conducted based on the epipolar geometric relationship (Hsiao et al. 2011; Fig. 3).

2. VBS-RTK technology

The VBS-RTK system is managed by the National Land Survey and Mapping Center (NLSC), Ministry of the Interior, Executive Yuan of ROC (Taiwan). The network uses continuous satellite observations and processes them continually. Users need to receive more than four GPS satellite signals to obtain high accuracy positioning coordinates in a short period of time. Fig. 4 shows the distribution of the entire VBS-RTK network, which consists of approximately eighty operational stations located around the main island and on most of the offshore islands.

Using the proposed unconventional photogrammetry method to reconstruct three-dimensional data requires knowing the relative coordinates of the object against the image coordinates. Reference control points are required in order to convert them into the commonly used TWD97 coordinates in Taiwan, and facilitate the follow-up overlapping with other data sets.

This study uses VBS-RTK, which can achieve real time positioning, in order to obtain the actual coordinates of reference control points. Due to the vigorous development of the Internet and wireless data communication transmission technology, GPS RTK has

become the mainstream of international surveying, mapping, and positioning technology. In particular, network VBS-RTK technology core positioning technology, which combines satellite positioning, broadband network data communication, Mobile Phone mobile data transmission, data storage, and a global information website for overall system applications and data supply dimensions, and has become the basis for the establishment of real time, high precision dynamic positioning systems under construction by advanced countries around the world.

The basic concepts of the VBS-RTK positioning technology are: multiple GPS base stations continuously receive satellite data, which connect to the control and computation center through a network or other communication equipment to produce a regional correction parameter database to calculate the relevant data of VBS close to any rover. Therefore, in the range of a baseline network, as formed by the base stations, the RTK user needs only to input the rover satellite positioning receiver and transmit relevant positioning information, via wireless communication transmission technology, into the control and computation center and calculate the VBS simulation observations. The VBS observations are then fed back in the RTCM (Radio Technical Commission. for Maritime Services) standard format to the rover satellite positioning receiver, for short baseline RTK positioning operation to obtain real time centimeter level positioning coordinates.

Satellite positioning base stations have been established across Taiwan. Any location, including the island of Taiwan, Green Island, Orchid Island, Penghu, Kinmen, and Matsu, where the signals of 5 GPS satellites can be received can be used to perform control and computation center for summary and computational processing. By real time transmission of continuous per second satellite observation data, users can achieve centimeter level high precision RTK in a very short period of time by wireless network services, such as GPRS.

3. Sediment disaster scale assessment

The comparison of the environmental elevation 3D reconstruction data of the disaster area, with the 3D data acquired before the disaster, shows the landslide volume; in general, the landslide volume is used to quantify the scale of the sediment disaster. Fig. 5 shows the schematic diagram, using current and prior elevation changes for comparison. If the gap between the current elevation and the prior elevations is negative, it denotes “sediment loss” from collapse or landslide; on the contrary, if the gap is positive, it denotes “sediment accumulation”. The gap, multiplied by the high precision elevation grid area, denotes the topographic changes of a single grid. The scale of the sediment disaster is the production of sediment in the disaster area. The calculation of sediment is the addition of the total sediment loss and the total accumulation of sediment.

4. Case Study

The Leye collapse in the Morakot typhoon disaster area and its surroundings were selected as the research area in this study. During the Morakot typhoon, there was heavy rainfall in the Tseng-Wen Reservoir watershed. The long term heavy rain triggered a large number of collapses and mudslides, causing damage to roads and bridges. The Leye collapse zone was one of the newly

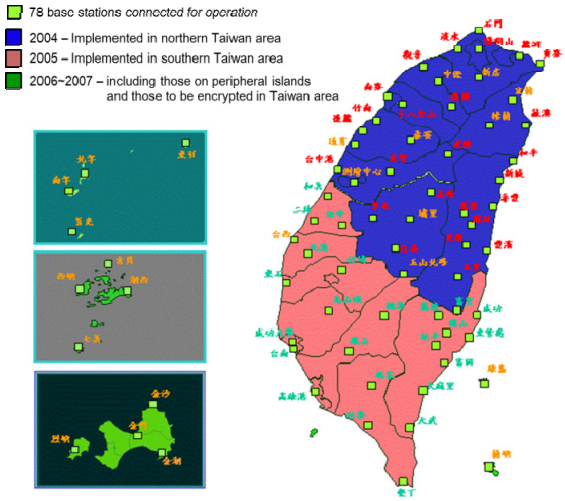

Fig.4 Distribution of VBS-RTK observation stations (Courtesy of NLSC, Taiwan)

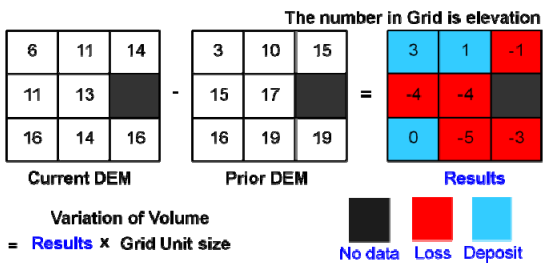

Fig.5 Calculation of Terrain Change (Hsiao et al. 2009)

collapsed regions caused by Morakot in the Tseng-Wen Reservoir watershed, and its collapse area is up to 90 hectares. As it borders on the Leye Tribe location and affects main roads, relevant authorities have invested governance funding. Below is the illustration of the UAV and VBS-RTK equipment, 3D reconstruction results, error matching, and sediment disaster scale assessment.

1. Research Equipment

Equipment includes photography and reference control points measurement equipment, as illustrated in sequence.

(1) Photography equipment:

- Remote control helicopter: engine displacement of 15cc, wood alcohol engine, weight of 4.8 kg, maximum load of 6 kg, fuel tank of 500cc, maximum flight duration of 30min, flight radius of 2-3km, and maximum flight altitude of 2-3km.
- Camera: Canon EOS 550D, valid pixel: 18 million, image size: 5184 × 3456 pixels, flash: 1/4000 second to 30 seconds.
- Lens: Canon EF 28mm f/1.8 USM, focal length: 28mm, maximum aperture: 1.8.

(2) Reference control points measurement equipment: this study used the VBS-RTK, manufactured by the German instrument maker Leica, for reference control points measurement, with the instrument specifications as shown in Table 1, and the appearance and measurement as shown in Fig. 6(a) and Fig. 6(b).

2. 3D reconstruction

UAV photography is a smaller range of photogrammetry, thus, there are few aerial photogrammetric targets, as shown in Fig. 7(a), for aerial survey in the surveyed area. To allow the UAV photography data to have a sufficient number of control points, more aerial photogrammetric targets need to be added. For the consideration of easy recognition in photos, this study constructed a thick white board, with a length and width at 2m as the aerial photogrammetric target, and attached the board with black tape to achieve grids of strong contrast, as shown in Fig. 7(b).

An experimental zone was selected at a landslide site in the Alishan area, where this study placed a total of 23 self-made aerial photogrammetric targets. The

Fig.6(a) VBS-RTK receiver and antenna (Model No.: Leica ATX1230 GG)

Fig.6(b) VBS-RTK on the ground control point

Table 1 Leica ATX1230 GG Specifications

No. of channels	12 L1 + 12 L2
L1 measurements	Carrier phase full wave length C/A narrow code
L2 measurements	Carrier phase full wave length with AS off or on P2 code / Pcode aided under AS Equal performance with AS off or on
Code and Phase Measurement Precision	
Carrier phase on L1	0.2mm rms
Carrier phase on L2	0.2mm rms
Code (pseudorange) on L1	2cm rms
Code (pseudorange) on L2	2cm rms
Accuracy (rms) with post processing	
Static (phase), long lines, long observations, choke ring antenna	Horizontal: 3mm + 0.5ppm Vertical: 6mm + 0.5ppm
Static and rapid static (phase) with standard antenna	Horizontal: 5mm + 0.5ppm Vertical: 10mm + 0.5ppm
Kinematic (phase), in movement mode after initialization	Horizontal: 10mm + 1ppm Vertical: 20mm + 1ppm
Accuracy (rms) with real-time/RTK	
Kinematic (phase), moving mode after initialization	Horizontal: 10mm + 1ppm Vertical: 20mm + 1ppm

experimental zone is as shown in Fig. 8. The 15 blue points are the reference points for coordinate conversion of 3D data. This study used 7-parameter Helmet transformation to process data. The 7-parameter Helmet transformation can reduce the scale errors. The remaining eight red points are the points for review after 3D data coordinate conversion. The yellow circle is the takeoff point of UAV as shown in Fig. 9. The red circle in the upper portion of the diagram is the self-made No. 12 aerial photogrammetric target, which can be easily recognized in the UAV photo. The central coordinates of each aerial photogrammetric target are measured by VBS-RTK, as shown in Table 2. Except for No. 6 point with a standard error at about 5cm, the standard error of other points is in the range of 2~4cm.

After recording 48 photos from multiple angles of the experimental zone, the SIFT algorithm was applied to extract the feature points and conduct image matching. Fig. 10 illustrates the schematic diagram of the UAV photographic achievements. Next, SfM was reused to obtain the camera parameters, while the multi-vision geometric approach was applied to obtain the 3D point cloud data with RGB color code. The results of 3D reconstruction are displayed by Trimble Realworks Survey 4.22, as shown in Fig. 11. In a total, 3,965,453 point cloud data with coordinates (TWD97_X, TWD97_Y, ellipsoid height) and codes of three primary colors (R, G, B) were produced. The average point cloud density is about 1.6 points/m^2. Since the range of the 3D reconstruction is about 2.5 square km^2, and the elevation of the experimental zone is in the range of 700 meters to 1300 meters, this study used 15 points for coordinated conversion to convert the 3D point cloud data from relative regional coordinates into a TWD97 coordinate system and ellipsoid height.

Fig.7(a) Common ground control point for aerial photogrammetry in Taiwan

Fig.7(b) Self-developed ground control point

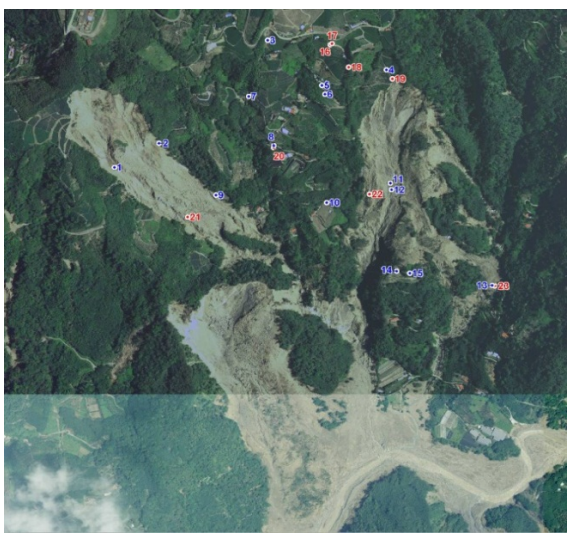

Fig.8 Testing area and control point distribution (Aug 2009)

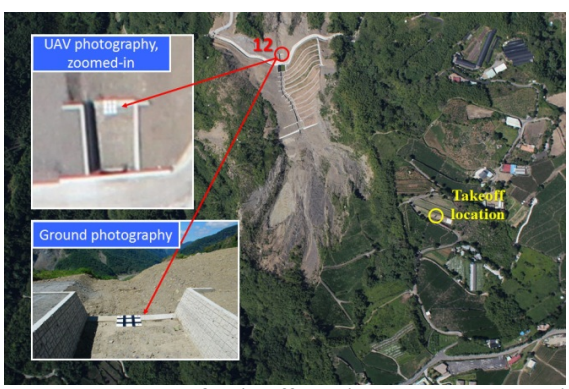

Fig.9 Location of takeoff in the testing area and No. 12 aerial photogrammetric target recognition schematic diagram

3. Three-dimensional reconstruction error comparison

After the coordinate conversion by the above method, this study compared the 3D reconstruction point cloud data and the data of other 8 points without coordinate conversion in terms of horizontal and elevation errors. The calculations of horizontal and elevation errors are as shown in Equations 4 and 5. The 3D reconstruction results' horizontal errors are in the range of 6.7 cm to 46.3 cm; the elevation errors are in the range of 0.14 meter to 1.09 meter (details are as shown in Table 3).

$$\text{Horizontal difference} = \sqrt{(X_1 - X_2)^2 + (Y_1 - Y_2)^2} \quad (4)$$

$$\text{Elevation difference} = |Z_1 - Z_2| \quad (5)$$

The point number (n) and error reliability (Er) equation as shown in Eq.6 (Li 1991), with reliability (R) more than 73.3% in this study (as shown in Eq.7).

$$E_r = \frac{1}{\sqrt{2(n-1)}} \times 100\% \quad (6)$$

$$R = 1 - E_r \quad (7)$$

4. Sediment disaster assessment

DTM of the study area before the disaster, at a resolution of 5 meters accuracy is ±2 m in horizontal and ±3 m in elevation (Chang et al. 2005). The 5m DTM are compared with the results of the UAV 3D reconstruction in order to identify areas where topographic elevation has changed and assess the major sources of sediments, potentially unstable areas, and the scale of the sediment disaster. The method proposed in section 3 was used to calculate the changes in the topographic elevations before and after disaster. The results are as shown in Fig. 12. The negative gap of changes in the elevation indicates the area of sediment loss, as represented in red. Therefore, the major sources of the sediment in this disaster are the upper edges of the three landslides, and the total loss of sediment is -5,841,987.75 m^3; the area of positive gap in the changes of elevation indicates the area of earthwork accumulation, namely, the area of accumulated landslide, as represented in blue. According to the analysis results, after the landfall of Morakot, the resultant landslide are mainly concentrated at the central and eastern landslide slopes. These unstable materials may move to the downstream area under the influence of the following torrential rains. In addition, some debris are concentrated on the lower edge of the landslide slope. Due to the steep landscape, the debris may fall due to wind, gravity, or rainfall, posing a threat to locals and requiring special concern in treatment. The total accumulated sediment amounts to

Fig.10 Testing area UAV photography results combination schematic diagram (June 2011)

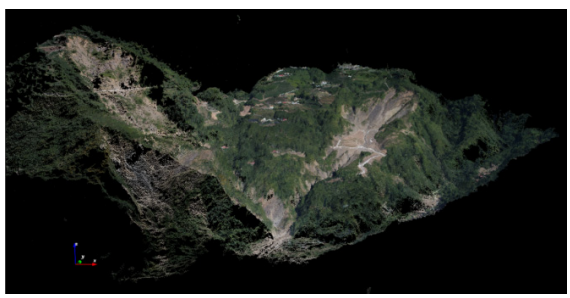

Fig.11 3D reconstruction results schematic diagram (the red, green, and blue arrows at the bottom on the left represent X, Y, and Z axis, respectively)

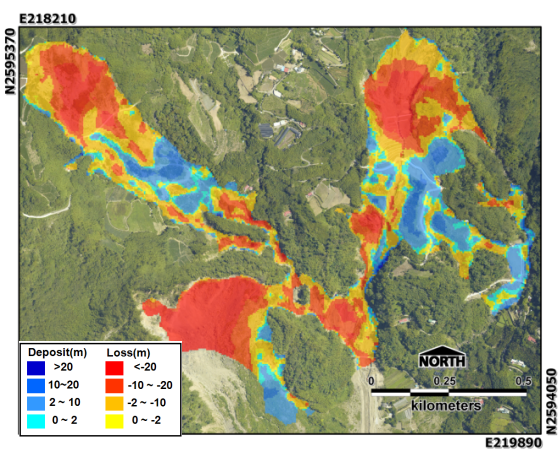

Fig.12 Calculation of changes in topographic change using the three-dimensional reconstruction results and pre-disaster DTM data

819,858.25 m^3; moreover, the sediment production by adding the total loss of sediment with the total accumulation of the sediment is -5,022,129.5 m^3, which can be used to assess the disaster scale of the area.

5. Conclusions

Unconventional photogrammetry does not require special measurement cameras and operates with few constraints. Additionally, it is more flexible, as historical photos or photos taken by any person after the disaster can be used. VBS-RTK is a rapid GPS positioning technology developed in recent years. This study used UAV to overcome the limitations of shooting angles in ground photography, and obtained the resulted point cloud data of 3D reconstruction by integrating VBS-RTK. The proposed technology is suitable for post-disaster damage information collection and historical three-dimensional environment reconstruction based on historical photos. In this study, the horizontal error is lower than 50cm and the elevation error is mostly below 1 meter. The integration of UAV photogrammetric photos and VBS-RTK for the rap id reconstruction of 3D information of the disaster area, is

Table 2 Coordinates of ground control target points and standard deviations

No.	TWD97_X	TWD97_Y	h (m)	Standard Deviation (m)	Purpose
1	218408.02	2595011.43	1161.24	0.022	Coordinate transformation
2	218573.27	2595106.05	1157.40	0.026	Coordinate transformation
3	218978.26	2595508.39	1160.86	0.035	Coordinate transformation
4	219420.24	2595392.96	1122.80	0.050	Coordinate transformation
5	219180.25	2595332.11	1117.22	0.032	Coordinate transformation
6	219191.10	2595297.91	1107.99	0.051	Coordinate transformation
7	218907.66	2595288.62	1078.06	0.042	Coordinate transformation
8	219000.64	2595096.11	1055.00	0.037	Coordinate transformation
9	218785.91	2594902.94	1017.60	0.020	Coordinate transformation
10	219197.35	2594874.21	964.71	0.024	Coordinate transformation
11	219434.43	2594949.71	961.18	0.026	Coordinate transformation
12	219439.25	2594924.47	953.64	0.019	Coordinate transformation
13	219813.77	2594550.55	791.64	0.027	Coordinate transformation
14	219458.09	2594606.38	895.17	0.033	Coordinate transformation
15	219507.34	2594598.33	901.42	0.022	Coordinate transformation
16	219210.87	2595490.94	1151.67	0.037	Error comparison
17	219217.21	2595494.94	1151.37	0.030	Error comparison
18	219279.78	2595402.84	1137.07	0.025	Error comparison
19	219442.13	2595357.57	1114.29	0.036	Error comparison
20	218998.99	2595089.82	1053.61	0.031	Error comparison
21	218680.58	2594817.43	1034.03	0.028	Error comparison
22	219356.78	2594906.54	961.58	0.027	Error comparison
23	219823.15	2594548.58	791.94	0.036	Error comparison

Table 3 Error comparison of point cloud and control points after 3D reconstruction

No.	GPS measurement value (a)			Value after coordinate transformation (b)			Horizontal Difference (m)	Elevation/vertical difference (m) $\lvert h_a-h_b \rvert$
	TWD97_X	TWD97_Y	h (m)	TWD97_X	TWD97_Y	h (m)		
16	219210.87	2595490.94	1151.67	219210.82	2595491.19	1151.81	0.24	0.14
17	219217.21	2595494.94	1151.37	219216.93	2595495.02	1152.46	0.29	1.09
18	219279.78	2595402.84	1137.07	219279.91	2595402.97	1137.69	0.19	0.62
19	219442.13	2595357.57	1114.29	219442.24	2595357.58	1114.75	0.11	0.46
20	218998.99	2595089.82	1053.61	218999.01	2595089.90	1053.33	0.08	0.28
21	218680.58	2594817.43	1034.03	218680.34	2594817.04	1034.97	0.46	0.94
22	219356.78	2594906.54	961.58	219356.71	2594906.49	960.73	0.09	0.85
23	219823.15	2594548.58	791.94	219823.11	2594548.63	791.51	0.07	0.43

very suitable for assessment of the scale of sediment disasters, including landslides and debris flows, which can effectively reflect the changes in topography in real time and provide reference in disaster relief responsive decision making in order to minimize disaster risks.

According to the experimental results of this study, the elevation error is greater than the horizontal error without direction. Hence, it is recommended that loca tions with great elevation difference should be selected as the aerial photogrammetric targets in order to improve elevation precision. The coordinate conversion of control points can also affect the coordinate results; hence, it is recommended to discuss changes in precision using different methods of coordinate conversion. Moreover, it is recommended to use UAV to take photos of disaster areas inaccessible to investigators (e.g., the other side of the canyon). By using VBS-RTK for dynamic positioning and 3D reconstruction point cloud technology, landslide and accumulation disaster preliminary assessment quantitative data can be established.

References

[1] 柯濤、張祖勛、郭大海、王建超 (2010)，「應急響應下的航空攝影測量」，2010 兩岸非常規攝影研討會，台南。(Ko, T., Zhang, Z.X., Guo, T.H., and Wang, C.C. (2010). “Aerial Photogrammetry in the Fast Response.” 2010 Workshop on Unconventional Photogrammetry, Tainan. (in Chinese))

[2] 孫明傳、段艷 (2010)，「基於最小二乘平差的區域網均色方法研究」，2010 兩岸非常規攝影測量研討會，台南。(Sun, M.C., and Duan, Y. (2010). “Research of Tone Balance Method With Least Squares Block Adjustment.” 2010 Workshop on Unconventional Photogrammetry, Tainan. (in Chinese))

[3] 張勇、柯濤 (2010)，「基於已有正射影像和 DEM 的航空攝影空中三角測量」，2010 兩岸非常規攝影測量研討會，台南。(Zhang, Y., and Ko, T. (2010). “Ortho Updating by Aerial Triangulation based on the Existing Ortho-photos and DEM.” 2010 Workshop on Unconventional Photogrammetry, Tainan. (in Chinese))

[4] 張國楨、陳俊愷、林姵伶 (2005)，「利用福衛二號立體影像對生產 DTM 之精度探討」，第三屆數位地球國際研討會，台北。(Chang, K.C., Chen, J.K., and Lin, P.L. (2005). “The Accuracy of DTM Generated by FORMOSAT-2.” The 3th Digital Earth Workshop, Taipei.(in Chinese))

[5] 蕭震洋、林伯勳、鄭錦桐、辜炳寰、徐偉城、冀樹勇 (2009)，「應用光達技術進行集水區土砂運移監測及攔阻率評估」，中興工程季刊，第 105 期，第 17-25 頁。(Hsiao, C.Y., Lin, B.S., Cheng, C.T., Ku, B.H., Xu, W.C., and Chi, S.Y. (2009). “Application LiDAR technology monitoring sediment transport and evaluate Sediment Delivery Ratio in watershed.” *Sinotech Engineering Journal,* 105, 17-25. (in Chinese))

[6] 蕭震洋、謝寶珊、冀樹勇 (2011)，「應用非常規攝影量測評估國道 3 號 3.1 公里崩塌事件之土方量」，中華水土保持學報，第 42 期，第 3 卷，第 120-130 頁。(Hsiao, C.Y., Hsieh, P.S., and Chi, S.Y. (2011). “Preliminary Study of Using Unconventional Photogrammetry to Evaluate the Earthwork Volume – a Case Study of the Landslide Occurred on the Cidu Section of Formosan Freeway.” *Journal of Chinese Soil and Water Conservation,* 42(3), 120-130. (in Chinese))

[7] 趙曉、黃潤秋、韋穗 (2004)，「基於計算機視覺的地形 3D 重建」，地質災害與環境保護，第 15 卷，第 2 期，第 74-77 頁。(Zhao, X., Huang, R.I., and Wei, S. (2004). “Reconstruction on 3D topography based on computer vision.” *Journal of Geological Hazards and Environment Preservation,* 15(2), 74-77. (in Chinese))

[8] Bertozzi, M., and Broggi, A. (1997). “Vision-based vehicle guidance. ” Computer, 30, 49-55.

[9] Broggi, A., Bertozzi, M., Fascioli, A., and Conte, G. (1999). Automatic Vehicle Guidance: The Experience of the ARGO Autonomous Vehicle, World Scientific Singapore.

[10] Bunke, H., and Wang, P. S. P. (1997). Handbook of Character Recognition and Document Image Analysis, World Scientific, Singapore.

[11] Chu, C.M., and Chien, Y.C. (2004). “New GPS Technology - Virtual Reference Station.” The 6th Symposium on GPS TechnologyTainan, Taiwan.

[12] Doermann, D. (1998). “The indexing and retrieval of document images: a survey.” Computer Vision and Image Understanding, 70(3), 287-298.

[13] Furukawa, Y., and Ponce, J. (2010). “Accurate, Dense, and Robust Multiview Stereopsis.” IEEE Transactions on Pattern Analysis and Machine Intelligence, 32(8), 1362-1376.

[14] Landau, H., Vollath, U., and Chen, X. (2004). “Virtual Reference Station Systems.” Journal of Global Positioning Systems, 1(2), 137-143.
[15] Li, Z. (1991). “Effects of Check Point on the Reliability of DTM Accuracy Estimates Obtained from experimental test.” Photogrammetric Engineering & Remote Sensing, 57, 1333-1340.
[16] Lowe, D.G. (1999). “Object Recognition from Local Scale-Invariant Features.” International Conference on Computer VisionCorfu, Greece, 1150-1157.
[17] Lowe, D.G. (2004). “Distinctive image features from scale-invariant Key points.” International Journal of Computer Vision, 60(2), 91-110.
[18] Lowe, D.G. (2007). “Automatic Panoramic Image Stitching using Invariant Features.” International Journal of Computer Vision, 74(1), 59-73.
[19] Masaki, I. (1992). Vision-based Vehicle Guidance, Springer-Verlag, New York.
[20] Snavely, N., Simon, I., Goesele, M., Szeliski, R., and Seitz, S.M. (2010). “Scene Reconstruction and Visualization from Community Photo Collections.” Proceedings of the IEEE., 98(8), 1370-1390.
[21] Sun, Z., Bebis, G., and Miller, R. (2006). “On-Road Vehicle Detection: A Review.” IEEE Transactions on Pattern Analysis and Machine Intelligence, 28(5), 694-711.
[22] Tomasi, C., and Kanade, T. (1991). “Detection and Tracking of Point Features." Carnegie Mellon University, Pittsburgh, PA.
[23] Wang, M.S., Liu, C.C., and Lee, Y.H. (2006). “Setting A Real-Time Kinametic (RTK) System of National e-GPS Base Staions.” M. o. I. National Land Surveying and Mapping Center, ed.
[24] Zhou, K. (2010). “Structure & Motion.” Institute of Computer Graphics and Algorithms, Pattern Recognition and Image Processing Group, Vienna.

2012 年 09 月 10 日　收稿
2012 年 11 月 17 日　修正
2012 年 11 月 27 日　接受
(本文開放討論至 2013 年 9 月 30 日)